Characterizing Spectral Response in Thermal Environments, the HYPSO-1 Hyperspectral Imager

Elizabeth Frances Prentice, Marie Bøe Henriksen, and Tor Arne Johansen
Center for Autonomous Marine Operations and Systems (AMOS)
Department of Engineering Cybernetics, Norwegian University of Science and Technology
7034 Trondheim, Norway

Fermín Navarro Medina and Alejandro Gómez San Juan
Departamento de Enxeñaría Mecánica, Máquinas e Motores Térmicos e Fluídos
Universidade de Vigo
36310 Vigo, Pontevedra, Spain

***Abstract*—The ocean color mission, HYPerspectral Smallsat for ocean Observation (HYPSO-1), required an instrument built with spectral measurement capability. Anticipated spectral signatures needed to provide sufficient detail of the target ocean surface within a defined spectral range (visible, near-infrared). The resulting instrument for this mission is a custom-built hyperspectral imager composed of both machined parts and Commercial Off-The-Shelf (COTS) components. Many of the COTS components lacked details on material composition, requiring additional testing and assumptions about their thermal properties. The imager was characterized through spectral and radiometric calibration, analyzed for stray light, and sized to fit a 6U CubeSat bus. However, issues with spectral response stability were noted during thermal-vacuum testing of the integrated satellite. In this paper we characterize the thermally-influenced spectral response of the imager using a thermal chamber and fluorescent lamp setup. Through a comparison of response spectra, we measure bandwidth, calculated as Full Width at Half Maximum (FWHM) of the spectral lines, at temperatures ranging from -20 to 50 degrees Celsius - the expected in-orbit operational range inside the CubeSat. It is apparent that bandwidth changes with rising imager temperature and peak spectral response shifts by a few nanometers depending on wavelength. This needed to be accounted for prior to launch as it will influence the results of planned ocean color analyses.**

In small satellites, passive thermal control systems can be constrained by limited physical space and efficiency; active solutions often suffer from limited power budgets on-board. Although the chosen passive thermal control solution for HYPSO-1 will remain in place, this characterization procedure can be used to aid in thermally calibrating data received from the satellite throughout the mission.

TABLE OF CONTENTS

978-1-6654-3760-8/22/$31.00 ©2022 IEEE

1. INTRODUCTION

The HYPerspectral Smallsat for ocean Observation (HYPSO-1) imager is a miniature transmissive grating hyperspectral instrument that records spectral data in the visible to near infrared wavelength range of $400-800$nm. It has a theoretical Full Width at Half Maximum (FWHM) of 3.33nm with 124 spectral bands. The imager is the primary payload on the HYPSO-1 mission, a 6U ocean color observation CubeSat developed at the Norwegian University of Science and Technology (NTNU). The imager has been delivered to the bus provider and the CubeSat is scheduled for launch in January 2022. HYPSO-1 is the first research satellite from NTNU, but more hyperspectral payloads are planned to follow in the coming years.

The HyperSpectral Imager (HSI) is designed to take images along the Norwegian coast from a 500km orbit in order to gather data on ocean color events such as algal blooms. The spectral signatures of algae vary, so sufficient spectral resolution is required to discern constituents of the water. The Committee on Earth Observation Satellites (CEOS) and International Ocean Colour Coordinating Group (IOCCG) recommend a minimum FWHM of 5nm for ocean color sensors [1], [2]. Therefore, it is important that the HSI is able to achieve such spectral resolution. During final testing in a Thermal Vacuum (TVAC) chamber, stability of the FWHM showed fluctuation with temperature. Many studies show spectral variation of temperature-dependent targets, such as in the agricultural and food sciences industry[3]. But in space, the temperature of the instrument itself can have even larger implications - and can be exposed to more extreme temperatures than imagers here on Earth. Hyperspectral instrument temperature-dependency was noted already with the Hyperspectral Imager for the Coastal Ocean (HICO) instrument on board the International Space Station in 2008 [4] where both the dark current and focal point of the lens were affected. These changes and shifts of the spectra in response to temperature not only can produce unexpected data, but also affect the way that the results are interpreted.

The HYPSO-1 payload is assembled using Commercial Off-The-Shelf (COTS) components so not much can be done to affect their resilience to temperature extremes, but there are several methods that can help control the thermo-mechanics through custom imager design. On Earth-based models such as telescopes, intentional gaps and adjustable lenses can be used to compensate for thermal expansion [5]. On space-based platforms it is often prohibitively difficult to make adjustments after launch, and usually better to limit moving parts all together. In this way, satellites rely on heating and cooling systems on-board that help regulate internal

temperatures [6], [7]. For CubeSats, or small satellites, power budgets are generally much smaller due to smaller surface areas for harvesting solar energy and less space for energy storage or batteries. This puts a limitation on active devices that can help regulate internal temperature. Regardless of the satellite size, thermo-optical design often features: careful material selection, multiple layers of insulation, mechanical isolation, and thermal straps connected to passive radiators or sinks [8], [9], [10], [11]. Active thermoelectric heating / cooling devices are also sometimes used even on smaller platforms, such as with the thermal imager on HyperScout [12]. Another common approach is to use as much of a single material in manufacturing as possible such that thermal expansion is uniform throughout the imager [13], called an athermal system.

On HYPSO-1, the thermal design includes several passive solutions since the power budget prohibits active heating or cooling. Although COTS components were used, the first design decision was to machine all remaining components from one Aluminum 6082 block. The platform base of the imager is bulky to serve as a high surface area heat sink (and rigid platform). Machined components were anodized black. Thermal straps mounted with thermal paste link heat sources, such as the camera head and electronics, to heat sinks, like the platform. With the thermal design fixed, there is still a remaining option for managing the temperature fluctuations and their effect on spectral data. As presented in Lucke et al.[4], pre- and post- calibration can be used to characterize the behavior and correct for it in the data, and this approach is what follows.

The objective of this study is to understand and characterize the spectral response of the HYPSO-1 CubeSat hyperspectral imager and its dependency on the thermal environment – before it is launched into orbit. In this paper we present the initial results from TVAC testing, a simplified setup for establishing a baseline of measurements, experimental results, and a method to model and compare the results. We also explore limitations of the experiment and discuss techniques for improving the study in the future. This work is intended as a preliminary study to investigate the changes in spectral response with temperature. The characterization will give an idea about the effects that can be expected with initial HYPSO-1 data and help to establish a baseline method for further measurements that can be used in future missions, such as HYPSO-2.

2. THE HYPSO-1 MISSION

The HYPSO-1 mission is a 6U CubeSat research project that will provide open-access hyperspectral image data with a focus on ocean color applications [14]. It will be launched into sun-synchronous, Low Earth Orbit (LEO) in January 2022 and has an estimated 5-year lifetime. Energy is harvested with external solar panels. Communication is over Ultra High Frequency (UHF) and S-band radio between the ground station at NTNU and the satellite. The primary payload of the CubeSat is a HSI that is designed based on COTS components and an in-house machined supporting structure [15]. Figure 1 illustrates the final design.

Model Strategy

Many iterations of the imager were developed throughout the course of the program. Three imagers of the final design, as shown in Figure 1, exist: (1) the Engineering Model (EM), (2) the Qualification Model (QM), and (3) the Flight

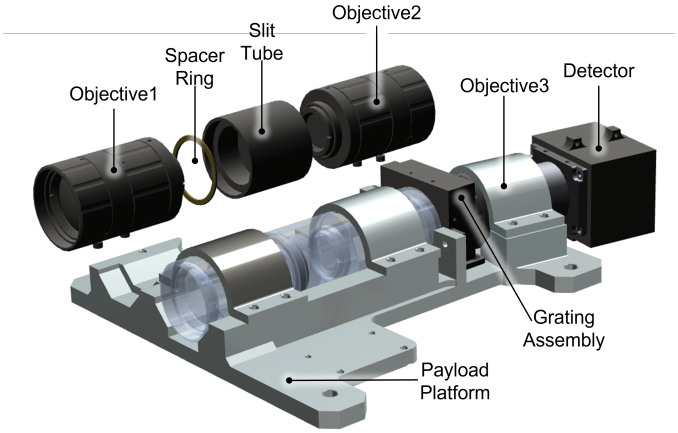

Figure 1. The HYPSO-1 hyperspectral imager highlighting the front optics assembly. Focus is adjusted manually by adding different thickness spacer rings between the front and collimating objectives (1-2).

Model (FM). The EM contains nearly all identical parts to its fellow models, except for a slightly older version of the slit tube. Its length was decreased for the QM and FM to achieve better focus. The QM and FM were additionally cleaned thoroughly with ultrasonics and fully assembled in a flowbench / cleanroom. The EM is used for testing in the lab, the QM for qualification testing, and the FM is for flight (after acceptance testing).

Design Considerations

The assembly of the optical train is not only sensitive to dust particles and contaminants, but also to precision tolerancing of manufactured parts. Using COTS components limits the control over tolerancing, which means that each imager must have custom settings to optimize focus and performance. The front optics in Figure 1 show the location of a spacer ring that can be used for fine-tuning. Various ring thicknesses will change the imager front focal length, in turn affecting the overall focus of the camera and the FWHM of the resulting spectral signal. In order to make scientific contributions to ocean color studies, a minimum FWHM must be met [1].

Anticipated Space Environment

Physically adjusting the spacing of the optics with the spacer ring can help set the focus, but this is dependent on the thermal environment. If the focus is set in ambient conditions in the lab, it will experience thermal expansion / contraction when exposed to other temperatures that can be expected in space. According to the satellite bus provider, internal temperatures could fluctuate from -40 to 70^oC worse case, or more likely, as simulated in Figure 2 throughout the course of one orbit (eclipse, nominal operation).

On the other hand, measured results from a 6U CubeSat of the same manufacturer show internal satellite temperatures ranging closer to 10 to 30^oC throughout the course of an orbit. Figure 3 shows the results of three sensors located inside the bus frame.

For this study, the focus will be on the operational temperature range of the satellite: -20 to 50^oC. This covers both the anticipated simulation results and the in-orbit measurements.

[1]NanoAvionics Corp., Vilnius, Lithuania, https://nanoavionics.com/

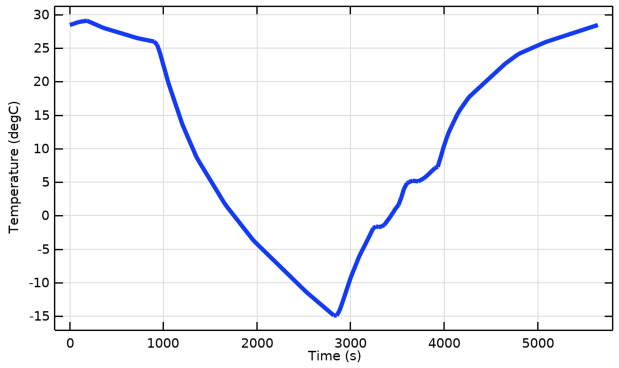

Figure 2. Simulated temperature profile measured on inside the HYPSO-1 CubeSat assuming nominal operations. Powered operations account for rising temperatures after eclipse. [source: NanoAvionics[1]]

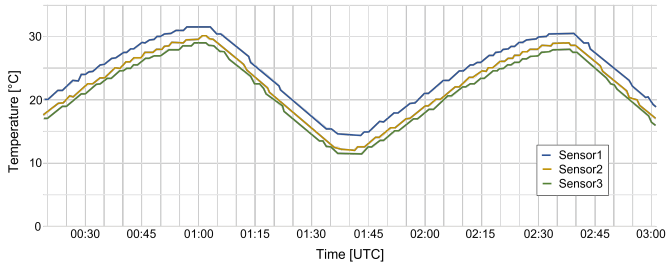

Figure 3. Measured in-orbit temperature profiles of 3 sensors located inside a NanoAvionics 6U CubeSat. [source: NanoAvionics[1]]

The non-operational, worse case range will not be covered since images are needed for an indication of performance. Although the expected thermal variation is within expected operating conditions on Earth, the fluctuation could possibly be enough to push the FWHM beyond the minimum mission requirement. This phenomenon became apparent after initial TVAC testing of the satellite QM.

3. Initial TVAC Results

The Assembly, Integration, and Testing (AIT) campaign for HYPSO-1 began with component and subsystem-level testing using various vacuum and thermal ranges. These tests were limited to facilities and machines available on-campus and/or inside the country during the covid-19 pandemic. Often, the machines could not meet the standardized testing requirements recommended by the European Space Agency (ESA) and the European Cooperation for Space Standardization (ECSS), for example [16]. Regardless, the initial results showed inconsistent spectral response with temperature, but the variation appeared minor. When the payload QM was completed, it was shipped out for testing in a TVAC chamber that was able to reach the qualification level testing requirements of the launch provider and tailored ECSS recommendations. During these tests, it was confirmed that the noted spectral response did, in fact, vary with chamber temperature in vacuum as well. This data necessitated a closer look into what was causing this variation in spectral response, how it could possibly be used to optimize imager performance, and what impact it had on the previously delivered FM imager scheduled for launch.

Device Under Test

The payload QM consisted of a HSI, a standard red-green-blue (RGB) imager, and the electronics stack (picoBoB) used to command the imagers. PicoBoB served as the interface between the satellite communication system / power bus and the payload. For this paper we consider only the performance of the HSI. The QM was built in-house and had previously been through a 72 hour bakeout prior to presented testing in the TVAC chamber.

Test Setup

The payload was mounted to an interface plate in the TVAC chamber facing the rear aluminum wall of the chamber. Temperature sensors were attached to critical components such as the sensor and front objective. A Multi Layer Insulation (MLI) blanket of $20+$ layers of aluminum foil was used to shroud the payload and protect the chamber, still leaving the imager an open view to the chamber wall. A single window was installed at the top of the chamber to illuminate the inside with a fluorescent light source. The lamp was mounted outside, fully covering the window. TVAC tests were run according to tailored ECSS standards / launcher requirements by cycling through temperatures between -20 and 50^{o}C while in 3×10^{-4} Pa vacuum. At defined Characterization Points (CPs), spectrograms (images captured by the sensor with spatial information on one axis and spectral information on the other) were taken of the illuminated chamber wall.

Spectral Response

The center line of each spectrogram taken at a CP was extracted and plotted in order to compare with responses at other CPs, Figure 4. The results are colored according to temperature - red for hot, blue for cold.

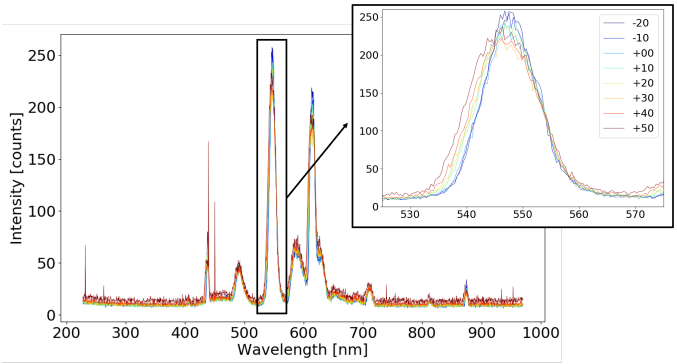

Figure 4. Spectral response of the QM HSI at varying temperatures inside the TVAC chamber: metallic chamber interior illuminated by an external fluorescent light source. The spectral peak at 546nm, a mercury emission line, is highlighted to show detail.

The signal is very noisy, especially for low signal returns. All data is below 250 counts out of a total saturation value of 4096. This means that the background noise accounts for a high percentage of the total signal. Additionally, the highly reflective aluminium interior of the chamber could be contributing as well. The noise level is much lower for the exact same imager when imaging a brighter, more Lambertian surface such as an optical calibration plate or integrating sphere. However, at least with the two highest peaks in the plot, there is about at 10% drop in signal strength with increasing temperature. The highlighted box in Figure 4 also shows a spectral shift with temperature change. The spectral

peaks shift approximately 3 pixels, corresponding to 1.15nm, from right to left with the increasing temperature from -20 to 50^oC. These results required further investigation.

4. Establishing a Baseline for Testing

The TVAC testing facility was located off-campus and testing was deemed non-mission critical - so beyond the budget. Therefore, an accessible, affordable alternative was needed. The SmallSatellite Lab at NTNU has unlimited and prioritized access to a thermal chamber (no vacuum) on campus. Since the spectral signal variation was noted both in preliminary thermal testing and full TVAC testing, this chamber was sought to provide a baseline setup for comparison.

Device Under Test

The QM tested in TVAC needed to remain in clean storage in case spare parts were needed for the FM prior to launch. This left the nearly identical EM available for testing. The EM and QM are the same in the sense that all COTS components have the same part number / manufacturer and machined components were made from identical source files. The one exception is that the slit tube length was shortened after issues with the EM focal length (the QM and FM slit tubes are the same). Either way, tolerancing can never be identical so there will always be differences in focus and overall performance. Thus, the results of the EM and QM cannot be directly compared, but should show correlation in spectral response.

Experimental Setup

A thermal chamber formed the basis of the experimental setup. The Vötsch VT 4011 (Vötsch Industrietechnik GmbH, Germany) chamber has an internal volume of 350 x 560 x 630 mm. Temperature can be controlled via the integrated interface screen from -40 to 180^oC. It was not possible to enable humidity control of the chamber for testing. An external sensor, the BME280 (Bosch Sensortec GmbH, Germany) with integrated Arduino UNO board (Arduino AG, Italy), was configured to record temperature, humidity, and pressure every 3 seconds inside the chamber. Instead of using the chamber outlet port only as a cable feed through, the HSI was positioned to 'look' through the chamber wall, and sealed off with Kapton® tape (DuPont de Nemours, Inc., USA). This enabled the imaging target setup to be moved outside of the chamber to isolate it from thermal effects. A simple cardboard box lined in white paper provided the simulated 'darkroom' target. A viewing port was cut to align with the HSI and black cloth was used to seal off external light from leaking in. A fluorescent bulb was inserted into the top of the box to provide a standard known signal for the imager to capture, similar to the bulb used in TVAC testing. It was turned on 30 minutes prior to testing. The setup is shown in Figure 5.

As with TVAC, temperatures were cycled through, this time from -20 to 50^oC, including a 30 minute dwell period once target temperatures were reached. After each dwell 10 spectrograms were taken. Center line plots, or spectra, were then plotted for comparison.

Confirming Spectral Response Fluctuations

The results of a ramp down (starting from 50 to -20^oC) test are shown in Figure 6. Even with the simplifications to the setup and test parameters, there is clear variation in the signal with respect to temperature. Since the new setup allowed for using white paper as a target and a direct light source, the noise is greatly reduced.

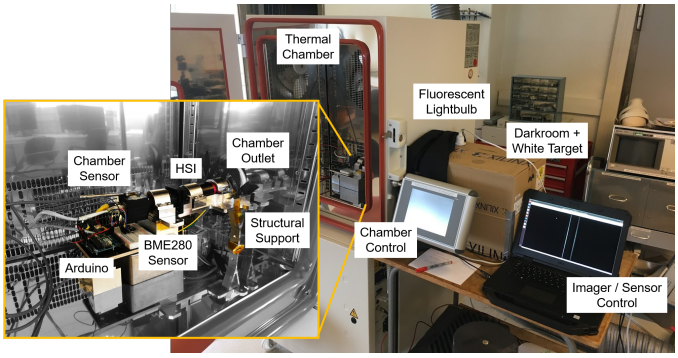

Figure 5. Test setup for the HSI in the thermal chamber.

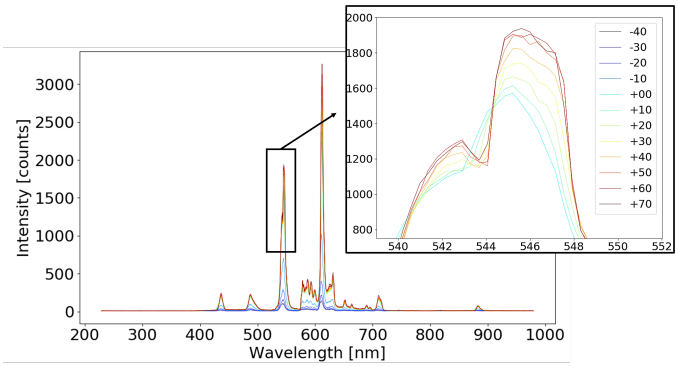

Figure 6. Spectral response of the EM HSI at varying temperatures inside the thermal chamber: external white paper target illuminated by an external fluorescent light source. Again, the 546nm mercury peak is highlighted and now shows it is a double peak with sufficient resolution.

As with the TVAC results, not only are intensities varying, but so is the spectral resolution (FWHM) as demonstrated by the double peak around 546nm - see subset image. At some temperatures within the operating range, it is almost impossible to discern the double peak signal. FWHM values from these thermal chamber results, compared with TVAC, are summarized in Table 1. Rather than using the double peak for comparison, the single peak at 611nm is studied.

Theoretically, as presented in Henriksen[17], the FWHM should be 3.33nm. Using the calibration setup for the FM, the measured FWHM fulfilled the mission requirement of less than 5nm. With both tests here though, results are much higher. This primarily has to do with the less precise experimental setup, and possibly due to different focus settings of the EM and QM. Lighting conditions were low even with high exposure times, the fluorescent light source does not have the same precise emission lines as calibration lamps, and the imaging target was not a calibration plate nor integrating sphere. With these improvements, a much lower FWHM could be expected.

Interestingly, signal intensities increased with temperature, while TVAC testing with the QM showed greater signal intensities with decreasing temperature. This was not expected since the EM and QM models were theoretically identical. As mentioned, though, individual imager focus can never be identical. If baseline model focus is different, thermal expan-

Table 1. Summary of FWHM values of the 611nm peak at varying temperatures for the QM in the TVAC chamber and the EM in the thermal chamber.

Temp. [degC]	TVAC Chamber, ramp-up [nm]	Thermal Chamber, ramp-up [nm]	Thermal Chamber, ramp-down [nm]
-20	9.68	8.76	6.66
-10	10.36	8.56	6.22
+00	11.18	8.43	6.11
+10	11.65	8.31	5.88
+20	12.51	8.19	5.70
+30	13.29	7.92	5.49
+40	13.76	7.72	5.32
+50	14.51	7.57	5.20
Average	*12.12*	*8.18*	*5.82*
Std. Dev.	*1.58*	*0.39*	*0.46*

sion / contraction could affect the signal response differently depending on whether focal lengths are slightly too long or too short to start. For example if the EM slit tube is too long, a shrinking effect would make the length more correct and therefore improve the spectral resolution (decreasing the FWHM). While if the QM slit tube already is too short, a shrinking effect would make the length even more wrong, giving worse spectral resolution (increasing the FWHM). This can explain why the two different trends of changes in FWHM are seen for the EM and QM.

As with TVAC results, a pixel shift of 2 pixels for ramp-up and 3 pixels for ramp-down, corresponding to 0.78nm and 1.17nm, respectively, is measured. This is interesting since it indicates that with or without vacuum, a similar change in thermal conditions will produce a similar shift in wavelength.

Both a ramp-up (-20 to 50^oC) and ramp-down (50 to -20^oC) temperature sequence was run in the thermal chamber with the same imager. Results look quite different, but this expected to considering the short, 30 minute dwell time. Without additional temperature sensors to verify component stability, it was difficult to establish a sufficient dwell. Increasing the dwell and soak times with additional sensors may bring ramp results closer. The notable feature in both the plots in Figure 7, though, is the extreme drop in signal sensitivity below around 0^oC.

This phenomenon did not occur during TVAC testing. The largest difference between the TVAC and thermal chamber setups is the air itself: pressure (vacuum) and humidity. Figure 8 shows readings from the independent temperature, humidity, pressure sensor inside the chamber for ramp-down measurements.

Not only do pressure and humidity change throughout the test, relative to temperature as expected, but also each day that a test is run, ambient conditions are different. It is very difficult to control these factors using the thermal chamber alone. In these plots it also shows that humidity rises with dropping temperatures. More water droplets in the air could be causing increased dispersion / reflection of light before it even reaches the imager. An attempt to mitigate this was to move the target outside of the chamber, see Figure 5, but it is still an unknown contribution.

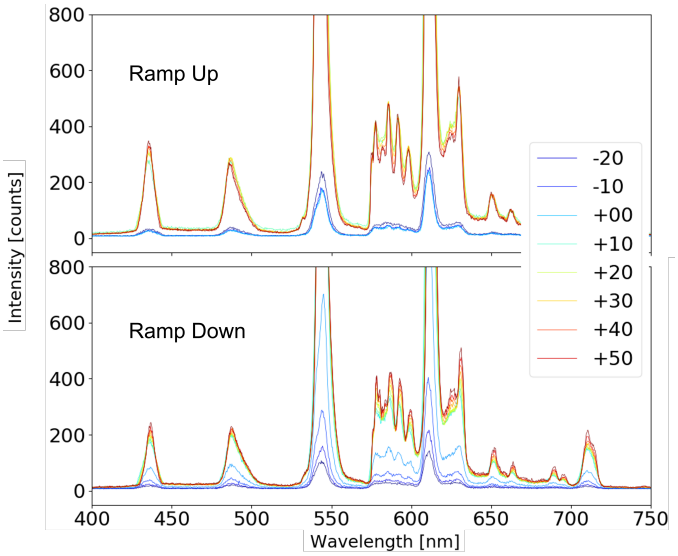

Figure 7. Highlighted low signal, subset of Figure 6 (both have the same temperature legend). Top plot shows results from ramping up chamber temperature, from -40 to 50^oC; bottom plot shows ramping down, from 70 to -40^oC.

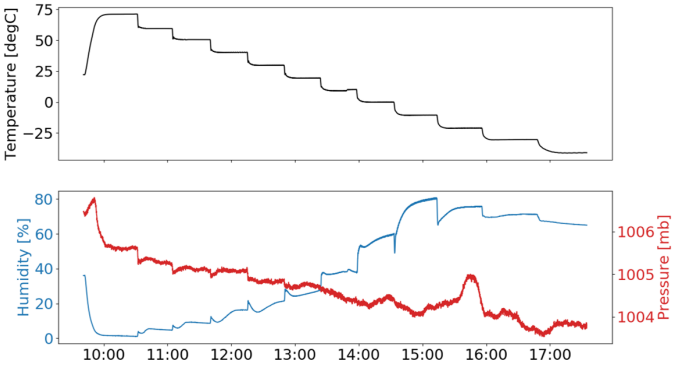

Figure 8. Temperature, humidity, and pressure readings from the Arduino BME280 sensor inside the chamber.

5. Experimenting with Opto-Mechanics

Each objective focus is set manually before assembling the imager. The imager focus can then be adjusted by varying spacer ring thickness as shown in Figure 1. This procedure requires extreme precision and accuracy and is prone to human error. After viewing preliminary thermal results, one thought was to use thermal testing to assist in setting imager focus and running a more accurate calibration (spectral and radiometric). The idea would be to select a baseline operating temperature expected in-orbit and to adjust the focus accordingly to achieve optimal performance. Focus can be more precisely targeted to a certain operational temperature environment this way, along with establishing the calibration parameters expected at varying temperatures. A second experiment was devised in order to evaluate how initial focal lengths affect the final spectrogram at varying temperatures, and also to investigate further the differing intensity responses

of the EM and QM.

This experiment follows the baseline experiment in every sense except that two cycles are run: one without a spacer ring and one with a spacer ring thickness of 3mm. If zoomed in on just the 611nm mercury peak highlighted above, the results look very similar (Figure 9). Both also look similar to the baseline testing of the EM that had a 1mm spacer ring.

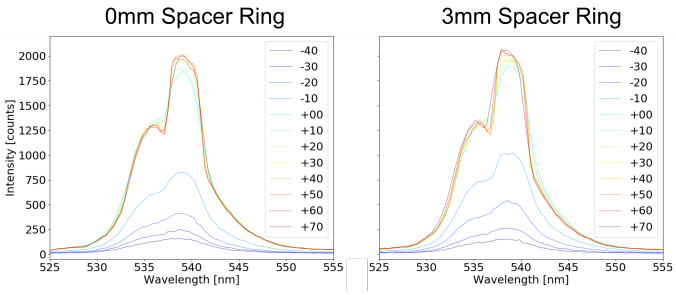

Figure 9. Spectral response of Terbium / Mercury peaks from ramp down thermal testing in the simplified thermal chamber: EM HSI with 0mm spacer ring (left) and 3mm spacer ring (right).

Figure 10 shows the result of plotting them together after spectral calibration. Compared, the spectra differ mostly in the lower temperature signal strength. This illustrates just how sensitive the imager is to a 3mm change in focal length, a reasonable displacement value for thermal expansion of aluminum (the main material used in the imager) within the temperature range tested.

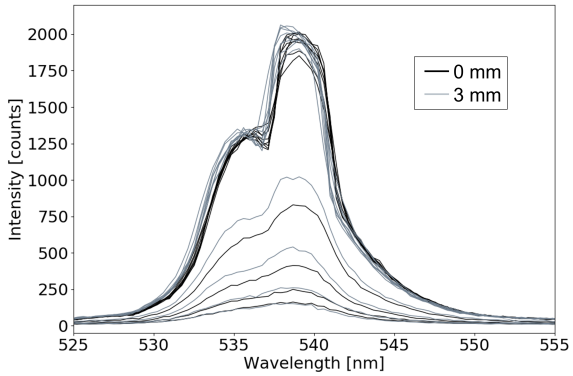

Figure 10. Comparison of spectral responses with varying spacer ring thicknesses.

This test highlights how initial imager configuration makes a difference in resulting spectrograms. Perhaps the best way to use this data is to 'build' the instrument in a TVAC chamber - or at least test configurations at varying temperatures to better define the optimal configuration for a target thermal environment.

6. Measuring Background Signal

Another consideration was to characterize the sensors background value readings with respect to changing thermal environments. As mentioned in Lucke et al.[4], Charge Coupled Device (CCD) sensors can be particularly sensitive to high temperatures. The HSI sensor is a Complementary Metal-Oxide Semiconductor (CMOS) sensor, but its background response to temperature, even within the operational range, was unknown. The baseline setup and EM were used for this experiment as described in Section 4 - the difference being that a lens cap was added and the imager was covered with black fabric to block any stray light inside the chamber. The window of the chamber was also covered with black paper.

Inside the Chamber

The first test was to record background values at various environmental temperatures such as those expected in-orbit as shown in Figure 3. A similar temperature profile was followed as with the baseline setup, and 10 spectrograms were taken at each temperature level, see Figure 11.

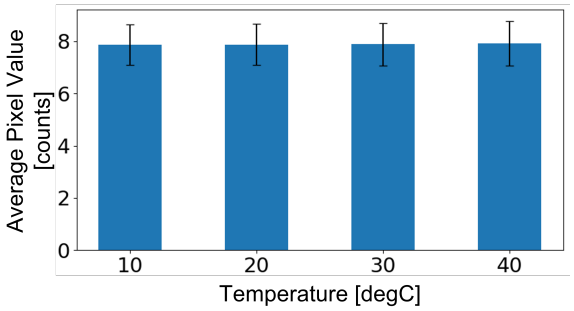

Figure 11. Average sensor background value measurements at various thermal chamber temperatures - average of 10 spectrograms. Error bars showing noise fluctuations of the background values for 10 spectrograms. Individual spectrogram results are comparable.

Total background value measurements vary from a minimum of 2 to a maximum of $35, 58, 133$, and 253 counts, respective to increasing chamber temperature, for all spectrograms taken in the series. However, spectrogram averages remain nearly constant with a highest average level of 7.91 counts and a standard deviation 0.85 at 40^{o}C. Saturation occurs at 4096 counts for a 12-bit imager, so the average background level change due to temperature fluctuations contributes to only around 0.2% of the total measured signal.

Inside the Sensor Housing

Additionally, temperature can be measured inside the HSI detector housing with a built-in sensor. When the camera is running, this internal temperature increases - roughly by about 10 degrees for a 1 minute run-time (and rises much more slowly after that). HSI imaging operations on-board the satellite are expected to last no longer than 57 seconds. This second test recorded images every $1 - 5$ minutes for about an hour while continuously running the camera in imaging mode. This was an attempt to also understand how internal temperatures affect the sensor and could possibly amplify the effect seen with external environment temperatures. Since operations are expected to take place with an internal satellite temperature between 10 and 30^{o}C, the thermal chamber was held constant at both of these temperatures while running the imager inside. Again, a lens cap and black fabric were used to block any light sources.

In both chamber temperature cases, sensor background values rise with increasing sensor temperature, see Figure 12. Noise fluctuations, or the standard deviation of the background values, vary from 0.78 to 0.80 counts in 10^{o}C and 0.83 to 0.91 counts in 30^{o}C. This shows a clear upward trend in

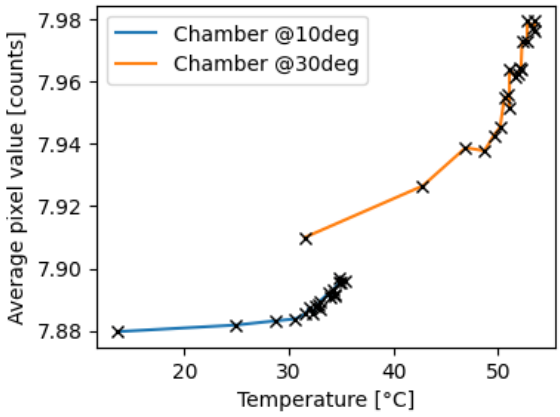

Figure 12. Average background value measurements at various internal imager temperatures. Results of the same test run inside the thermal chamber at 10 and 30^oC. Line plotted to distinguish chamber temperatures.

both average pixel value and fluctuation with temperature. Keeping the sensor cool inside the satellite and keeping operation time short will minimize background levels due to thermal effects. Overall, an increase of less than 1 count on average was measured within the expected operational temperature range. This amount of variation did not warrant mitigation measures nor design changes for the mission, but if used as a characterization, can provide additional accuracy for radiometric calibration once the imager is in orbit.

7. Modeling TVAC Results from Thermal Chamber Measurements

The uncertainties in spectrogram interpretation come from a myriad of mechanical, geometrical, and thermal properties of the components and assemblies. Each parameter contributes to the overall thermal, structural, and thermoelastic analysis, and they all depend on one another. This changes through design, manufacturing, assembly, testing, and eventually flight. Together, the parameters make predictions of the thermoelastic influence on the optical behavior of an instrument. Analyzing the exhaustive list of influences on-board a spacecraft is both infeasible and unreliable within the context of a time-limited university CubeSat project. However, some optical behavior predictions can be done by means of thermal testing.

To compare the spectra peaks obtained in both chambers, a conversion methodology is proposed. The understanding of the parameters that influence the differences will help to make the optical predictions mentioned. Here, the spectra from the TVAC chamber are assumed to be the reference, and the spectra in the thermal chamber are the results to be corrected. For the peak n, the ratio of maximum values (I_{mn}) and mid-peak wavelength (λ_{mn}) bewteen the TVAC (subscript $m = 0$) and thermal chambers (subscript $m = 1$) is as follows:

$$r_I = \frac{I_{0n}}{I_{1n}} \tag{1}$$

$$r_\lambda = \frac{\lambda_{0n}}{\lambda_{1n}} \tag{2}$$

In the thermal chamber, ramp-up and ramp-down tests were performed, so the average values for the spectra intensity is calculated as

$$I_1 = \frac{I_{lo2hi} + I_{hi2lo}}{2} \tag{3}$$

From the spectra in the thermal chamber, we correct the peak intensity and wavelength values to locate the maximum point of the peak in the same position than TVAC tests:

$$I_2 = I_1(\lambda')r_I \tag{4}$$

$$\lambda' = \lambda r_\lambda \tag{5}$$

Finally, to correct the wavelength width of each peak, the spectra intensity is manipulated according to

$$I_3 = I_2[1 + (\lambda' - \lambda_{0n})^{p_u} k_u] \quad \text{if} \quad \lambda' > \lambda_{0n} \tag{6}$$

$$I_3 = I_2[1 - (\lambda' - \lambda_{0n})^{p_l} k_l] \quad \text{if} \quad \lambda' < \lambda_{0n} \tag{7}$$

The intensity at half maximum of the peak

$$I_3(\lambda' = \lambda'_{FWHM}) = I_{0n}/2 \tag{8}$$

is used to equate the spectra of both tests, so that

$$K_u = \frac{1}{(\lambda'_{FWHM} - \lambda_{0n})^{p_u}} \left[\frac{I_{0n}}{2I_2(\lambda'_{FWHM})} - 1\right] \tag{9}$$

and

$$K_l = \frac{1}{(\lambda'_{FWHM} - \lambda_{0n})^{p_l}} \left[\frac{I_{0n}}{2I_2(\lambda'_{FWHM})} - 1\right] \tag{10}$$

are the multiplicative factors for $\lambda' > \lambda_{0n}$ and $\lambda' < \lambda_{0n}$, respectively. An example of the peak fitting is illustrated in Fig. 13, with the peak at the wavelength of 615 nm at 10ºC.

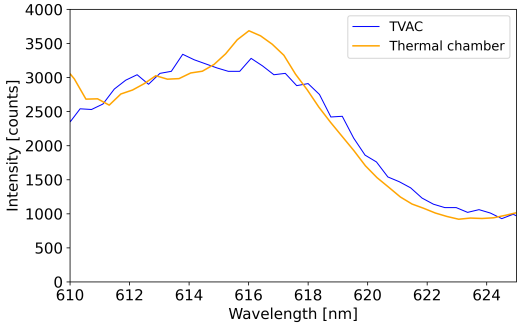

Figure 13. Peak at 611nm for 10^oC in TVAC chamber, compared with the corrected spectra for the same peak in the thermal chamber.

For the TVAC and thermal setups used in this paper, too many parameters varied simultaneously to be able to extract

any thermoelastic properties from the conversion between the TVAC and thermal datasets. For future tests this is, however, a useful method to compare the data if the setups have less varying factors (such as the lamp set-up, targets, light level etc.). With further dedicated tests, the parameters included in the conversion method r_I, r_λ, p_u, p_l, K_u, and K_l will be characterized as a function of the test factors.

8. Discussion and Future Work

Test how you fly. The setup and conditions of the experiments were not ideal, but were completed in the hope of finding a simplified solution that would make thermal testing more accessible to smaller CubeSat teams. Ideally these tests would have been done on a HSI model identical to the FM (such as the QM) in a TVAC chamber that could simulate the thermal *and vacuum* conditions that are expected in orbit. This is actually planned for HYPSO-2, at least in the sense of obtaining a TVAC chamber at the university. Another major limitation of this experiment was the selection of calibration targets: namely white paper and a fluorescent light bulb. Standardized calibration lamps, such as radiometric and spectral sources certified by the National Institute of Standards and Technology (NIST), and white Spectralon® (Labsphere / Halma PLC Group, UK) plates or an integrating sphere would further improve measurements of the FWHM and spectral calibration. If testing could be fully automated or controlled remotely, it would be better to increase soak and dwell times to ensure that the temperature of all imager components has stabilized before spectrograms are taken. Additional sensors inside the chamber would be required for this. If further experimentation continues with this thermal chamber, more work should go into controlling humidity in the chamber and sealing off inlets such as the cable feed through.

While many results proved similar between the TVAC and thermal chambers, not every measure could be scaled. Another possibility would be to look into modeling humidity effects on the optics by varying the refraction index in an optical modeling software, such as Zemax OpticStudio (Ansys, USA). This is particularly interesting to follow up with if an imager is to be designed for use on other planets with an atmosphere - for the sake of HYPSO-1, testing in a controlled TVAC chamber would best simulate future scenarios. Total background measurements could be improved by looking more closely into hot pixels values to possibly provide an indication of sensor temperature as demonstrated in Porter et al.[18]. Alternately, several studies, such as with Kim et al.[19], demonstrated adding strain gauges to components in order to measure actual thermal deformation in TVAC. Since the payload platform is thermally decoupled from the rest of the satellite via isolating dampers, thermoelastic deformation differentials can cause increased stress build-up at interfaces. Strain gauge measurements could help characterizing the current design and give hints for design improvements based on analyzing the most affected components.

9. Conclusion

This study concludes a preliminary survey of thermal effects on hyperspectral data anticipated for the HYPSO-1 CubeSat mission. The hyperspectral imager is a primarily COTS assembly, which leads to uncertainties about thermal properties and constituent materials. This means low confidence in our thermal models. Thus the study aimed to experimentally measure thermal effects and to provide methods for using those results to improve design and modeling.

The experimental investigation highlighted that HSI response is sensitive to ambient environmental temperature and humidity. In space-simulated environmental conditions, testing temperatures ranged from -20 to 50^oC in vacuum. Under these conditions, the spectra shifted an average 3 pixels (corresponding to about 1.15nm) and the FWHM changed by 4.83nm. Similar results were found with a simplified thermal chamber setup not including vacuum (pixel shift of 3 pixels and FWHM change of 1.46nm). With a mission requirement of a maximum of 5nm FWHM, this is a significant change. Considering the results were repeatable in a thermal chamber, spectral variation is likely linked to changing environmental temperature and a thermal chamber could be used to further study the thermoelastic response of the imager. However, signal at low temperatures was greatly reduced and is thought to be due to humidity in the air.

Another test demonstrated just how sensitive the optical train is to millimeter offsets. When the front objective was offset by 3mm, a roughly 200 count signal intensity change was noted at lower temperatures. Similar changes were seen for offsets of just 1mm. If the aluminium parts in the optical train expand or contract unevenly by this same amount over the expected temperature range, the effect will be visible in the spectral data. This finding can used in the design phase to help calibrate the imager based on producing optimal performance at the expected operational temperature.

Finally, background signal and noise fluctuations were measured at the same varying temperature ranges. The dark images showed that both the average background value and noise fluctuations increase with imager run-time (temperature) and environmental temperature. However, within expected operational conditions of $10 - 30^o$C and 1 minute of imager run-time, variation in the average background value was less than 1 count. Thus the background signal and noise fluctuations are not expected to play a significant role in a changing thermal environment.

Acknowledgments

The work is partly sponsored by the Research Council of Norway through the Centre of Excellence funding scheme, project number 223254 (NTNU-AMOS) and IKTPLUSS project MASSIVE with project number 270959 (NFR), the Norwegian Space Agency, and the European Space Agency (PRODEX - 4000132515). The authors would especially like to thank Tuan Tran, Tord Hansen Kaasa, Henrik Galtung, Martine Hjertenæs, Glenn Angell, and Terje Mathiesen for their help with design work, prototyping, software, and documentation of the process. Also to Lev Son and the NanoAvionics team, the HYPSO-1 bus provider, for data on the thermal environment in space and numerous conversations on thermal design from the beginning.

References

[1] CEOS, "Feasibility study for an aquatic ecosystem earth observing system," Committee on Earth Observation Satellites, CSIRO Canberra, Australia, Eds. Dekker, A.G. and Pinnel, N., Tech. Rep., 2018.

[2] IOCCG, "Earth observations in support of global water quality monitoring," International Ocean Colour Coordinating Group Report Series, No. 17, Dartmouth,

Canada, Eds. Greb, Steven and Dekker, Arnold and Binding, Caren, Tech. Rep., 2018.

[3] X. Xu, L. Xie, and Y. Ying, "Factors influencing near infrared spectroscopy analysis of agro-products: a review," *Frontiers of Agricultural Science and Engineering*, vol. 6, no. 2, 2019.

[4] R. L. Lucke, M. Corson, N. R. McGlothlin, S. D. Butcher, and D. L. Wood, "The Hyperspectral Imager for the Coastal Ocean (HICO): fast build for the ISS," in *Proc. SPIE 7813, Remote Sensing System Engineering III*, ser. 78130D, 26 August 2010.

[5] J. J. Gonzalez, C. Tejada, A. Farah, J. L. Rasilla, and F. J. Fuentes, "Thermal effects and thermal compensation in the OSIRIS camera," in *Proc. SPIE 4841, Instrument Design and Performance for Optical/Infrared Ground-based Telescopes*, 7 March 2003.

[6] E. Gorman, D. A. Kubalak, D. Patel, A. Dress, D. B. Mott, G. Meister, and J. Werdell, "The NASA Plankton, Aerosol, Cloud, ocean Ecosystem (PACE) mission: an emerging era of global, hyperspectral Earth system remote sensing," in *Proc. SPIE 11151, Sensors, Systems, and Next-Generation Satellites XXIII*, ser. 111510G, 10 October 2019.

[7] M. A. Folkman, J. Pearlman, L. B. Liao, and P. J. Jarecke, "EO-1/Hyperion hyperspectral imager design, development, characterization, and calibration," in *Proc. SPIE 4151, Hyperspectral Remote Sensing of the Land and Atmosphere*, 8 February 2001, pp. 40–51.

[8] J. Kurihara, Y. Takahashi, Y. Sakamoto, T. Kuwahara, and K. Yoshida, "HPT: A High Spatial Resolution Multispectral Sensor for Microsatellite Remote Sensing," *Sensors (Basel)*, vol. 18, no. 2, 2018.

[9] B. Sang, J. Schubert, S. Kaiser, V. Mogulsky, C. Neumann, K. P. Förster, S. Hofer, T. Stuffler, H. Kaufmann, A. Müller, T. Eversberg, and C. Chlebek, "The EnMAP hyperspectral imaging spectrometer: instrument concept, calibration, and technologies," in *Proc. SPIE 7086, Imaging Spectrometry XIII*, ser. 708605, 27 August 2008.

[10] D. Labate, M. Ceccherini, A. Cisbani, V. De Cosmo, C. Galeazzi, L. Giunti, M. Melozzi, S. Pieraccini, and M. Stagi, "The PRISMA payload optomechanical design, a high performance instrument for a new hyperspectral mission," *Acta Astronautica*, vol. 65, no. 9-10, pp. 1429–1436, 2009.

[11] M. Cutter and D. Lobb, "Design of the compact high-resolution imaging spectrometer (CHRIS), and future developments," in *Proc. SPIE 10568, International Conference on Space Optics — ICSO 2004*, ser. 1056805, 2017.

[12] M. Esposito, S. S. Conticello, M. Pastena, and B. Carnicero Dominguez, "In-orbit demonstration of artificial intelligence applied to hyperspectral and thermal sensing from space," in *Proc. SPIE 11131, CubeSats and SmallSats for Remote Sensing III*, ser. 111310C, 30 August 2019.

[13] P. Buschkamp, B. Sang, P. Peacocke, S. Pieraccini, M. J. Geiss, C. Roth, V. Moreau, B. Borguet, L. Maresi, M. Rast, and J. Nieke, "CHIME's hyperspectral imaging spectrometer design result from phase A/B1," in *Proc. SPIE 11852, International Conference on Space Optics — ICSO 2020*, ser. 118522K, 11 June 2021.

[14] M. E. Grøtte, R. Birkeland, E. Honoré-Livermore, S. Bakken, J. L. Garrett, E. F. Prentice, F. Sigernes, M. Orlandić, J. T. Gravdahl, and T. A. Johansen, "Ocean color hyperspectral remote sensing with high resolution and low latency — the HYPSO-1 CubeSat mission," *IEEE Transactions on Geoscience and Remote Sensing*, pp. 1–19, 2021.

[15] E. F. Prentice, M. E. Grøtte, F. Sigernes, and T. A. Johansen, "Design of a hyperspectral imager using COTS optics for small satellite applications," in *Proc. SPIE 11852, International Conference on Space Optics — ICSO 2020*, ser. 1185258, 11 June 2021.

[16] European Space Agency - TEB, "TEC-SY/128/2013/SPD/RW Tailored ECSS engineering standards for in-orbit demonstration CubeSat projects," 2016, issue 1, Revision 3.

[17] M. B. Henriksen, E. F. Prentice, T. A. Johansen, and F. Sigernes, "Pre-launch calibration of the HYPSO-1 cubesat hyperspectral imager," in *Proc. IEEE Aerospace*, 2021, [pending acceptance].

[18] W. C. Porter, B. Kopp, J. C. Dunlap, R. Widenhorn, and E. Bodegom, "Dark current measurements in a CMOS imager," in *Proc. SPIE 6816, Sensors, Cameras, and Systems for Industrial / Scientific Applications IX*, ser. 68160C, 29 February 2008.

[19] H.-I. Kim, J.-S. Yoon, H.-B. Kim, and J.-H. Han, "Measurement of the thermal expansion of space structures using fiber bragg grating sensors and displacement measuring interferometers," *Measurement Science and Technology*, vol. 21, no. 8, 2010.

BIOGRAPHY

Elizabeth Frances Prentice *is a PhD researcher in the Department of Engineering Cybernetics at the Norwegian University of Science and Technology (NTNU). She is researching optical remote sensing and mechanical integration for small satellites and robotic agents. She has been responsible for hardware development and assembly / integration / testing (AIT) on the HYPSO-1 CubeSat mission at NTNU. She earned a MSc in Applied Earth Science from TU Delft (Delft, the Netherlands, 2016), a BSE in Aerospace Engineering from the University of Michigan (Ann Arbor, MI USA, 2011), and has several years experience in dimensional engineering at a design-for-manufacturing consultancy firm.*

Marie Bøe Henriksen *received her M.Sc. degree in Engineering Cybernetics at the Norwegian University of Science and Technology (NTNU) in 2019, and is currently pursuing her PhD related to hyperspectral imaging in drones and small satellites with the same department. She is focusing on calibration and characterization activities with small and low-cost hyperspectral imagers. Her research interests include laboratory calibration methods, optical characterization set-ups, stray light and second order light correction, and smile and keystone correction.*

Tor Arne Johansen *received the MSc degree in 1989 and the PhD degree in 1994, both in electrical and computer engineering, from the NTNU, Trondheim, Norway. From 1995 to 1997, he worked at SINTEF as a researcher before he was appointed Associated Professor at the NTNU in Trondheim in 1997 and Professor in 2001. He has published several hundred articles in the areas of control, estimation and optimization with applications in the marine, aerospace, automotive, biomedical and process industries. In 2002 Johansen co-founded the company Marine Cybernetics AS where he was Vice President until 2008. Prof. Johansen received the 2006 Arch T. Colwell Merit Award of the SAE, and is currently a principal researcher within the Center of Excellence on Autonomous Marine Operations and Systems (NTNU-AMOS) and director of the Unmanned Aerial Vehicle Laboratory at NTNU and the SmallSat Laboratory at NTNU. He recently co-founded the spin-off companies Scout Drone Inspection, UBIQ Aerospace, Zeabuz and SentiSystems.*

Fermín Navarro Medina *received his PhD degree in 2010 and is a professor at the University of Vigo where he teaches several courses within the fields of aerodynamics and spacecraft, in the degree of aerospace engineering at the School of Aerospace and Space Engineering. He is the author of several publications and speaker at many national and international conferences in the field of spacecraft subsystems design. He has participated as thermal engineer in several missions of the European Space Agency (ExoMars, and Solar Orbiter). He is currently working on several space projects like Wiptherm, "Innovative Wireless Power Devices Using Micro-Thermoelectric Generators arrays", and on a lunar rover in the conceptual design phase.*

Alejandro Gómez San Juan *B.Sc. in Aeronautical Engineering (2010), M.Sc. degree (2013) and Ph.D. (2018) in Aerospace Engineering from the Technical University of Madrid (UPM - Universidad Politécnica de Madrid) in Spain. He is assistant professor and full-time researcher at University of Vigo. His research focuses on space systems, mainly in thermal control and mechanical engineering. Dr. Gomez-San-Juan has participated in a number of international scientific missions, such as ESA Solar Orbiter, ExoMars-2018, CNSA Chang'E 4 or UPMSat-2 in the framework of H2020 program of the EU.*